ELECTRONIC SUPPLEMENTARY INFORMATION

Nanoparticles Alter Locust Development and Behaviour

Preetam Kumar Sharma[1,3], Liya Wei[2], Atul Thakur[4] Jialing Pan[2], Chang Chen[2], Navneet Soin[1,5,6] Le Kang[2*], Nikhil Bhalla[1,7*]

[1]*Nanotechnology and Integrated Bioengineering Centre (NIBEC), School of Engineering, Ulster University, Belfast, York Street, Northern Ireland BT15 1AP, United Kingdom*

[2]*Institute of Life Science and Green Development / College of Life Science, Hebei University, Baoding 071000, China*

[3]*Institute for Materials Discovery, University College London, Malet Place, London WC1E 7JE, United Kingdom*

[4]*School of Electronics and Information Engineering, Nanjing University of Information Science & Technology, Nanjing, 210044, China*

[5]*School of Science, Computing and Engineering Technologies, Swinburne University of Technology, P.O. Box 218, Hawthorn Victoria 3122, Australia*

[6]*School of Science, RMIT University, Melbourne, Victoria 3001 Australia*

***Corresponding address: lkang@ioz.ac.cn; n.bhalla@ulster.ac.uk**

Table of Contents

Nanoparticle preparation and characterisation

Nickel ferrite, $NiFe_2O_4$ nanoparticles, were synthesised using a coprecipitation method. High purity nickel chloride hexahydrate (purchased from Merck/Sigma Aldrich, UK) and iron (III) chloride hexahydrate (purchased from Merck/Sigma Aldrich, UK) were combined in appropriate stoichiometric ratios and dissolved in a boiling solution of 0.40M NaOH (purchased from Merck/Sigma Aldrich, UK) under vigorous stirring for 30 minutes. Following cooling to room temperature, the resulting suspension underwent thorough washing with distilled water until reaching a pH of 7, followed by centrifugation to isolate the residue. This residue was then dried in an electrical oven at 50°C overnight (24 hours). Subsequently, the powders were subjected to calcination in a muffle furnace at 800°C for 3 hours, with a heating and cooling rate of 200°C per hour (Grieve, HD-183618-HT Electric). In Figure S1, we provide nanoparticle characterisation using X-ray diffraction(XRD), raman spectroscopy, scanning electron microscopy (SEM) and transmission electron microscopy (TEM) techniques.

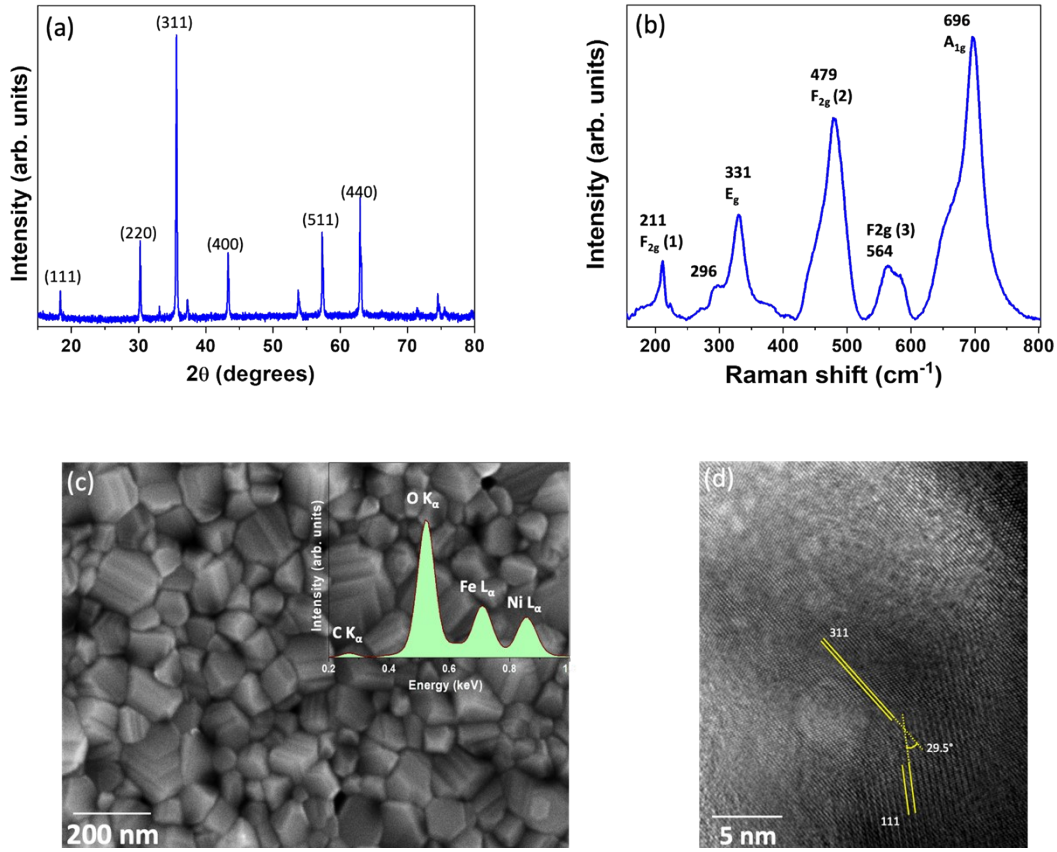

Figure S1. (a) X-ray diffractogram, (b) Raman spectrum (c) Scanning electron microscopy with inset showing the energy dispersive X-ray spectrum and (d) high resolution transmission electron microscopy image of the synthesized nickel ferrite MNPs.

Physicochemical characterisation of MNPs (SEM-EDX, Raman, TEM and XRD)

Nanoparticles were characterised by a variety of techniques. Scanning electron microscopy-energy dispersive X-ray analysis (SEM-EDX) was performed on Hitachi SU5000 field emission SEM coupled with Oxford Instruments EDX detector in low vacuum mode using back scattered electron detector at 10 kV. Transmission electron microscopy measurements were performed at 200 kV using Jeol JEM-2100f system. Raman spectroscopy measurements were performed using Renishaw inVia Qontor® spectrometer using 785 nm laser. Powder X-ray diffraction measurements were performed in the locked-couple mode in 10-80° range using Panalytical Empyrean Series 3 system.

Locust eggs handing, experiment preparation and characterisation

The eggs were received in jars filled with sand from Darwin Biological, UK. The silver sand was prepared by washing repeatedly under the tap water followed by drying in a saucepan with occasional stirring. Once dried and cool, 15 wt% water was added to the sand and mixed thoroughly. The moist sand is then transferred to a cylindrical jar (10 cm length and 5 cm diameter). Some images of eggs in jar and the condition of eggs within sand are shared in Figure S2.

Figure S2. Images of jar and egg pods, as labelled. The diameter of 20 pence coin (UK currency) is 21.4 mm, used for scale.

General observation on the received jars

For every batch two jars containing 2-3 egg pods (mostly two, except one jar from batch 3) were received (figure 1) from Darwin Biological, UK. The pods were buried approximately 7-10 cm deep and contained around 50-70 eggs. The eggs were of ellipsoidal in shape, 5-7 mm in length and 1-2 mm in diameter. On the bottom of every egg, germinal disk was visible.

Locust egg incubation

Two incubators, one humid (purchased from Medline Scientific, UK MDH2200-HC-E) and one dry (purchased from Medline Scientific, UK 26015, IB-01E Incubator (65L)); both maintained at 30°C, were being used for keeping eggs and hatchlings. The wet incubator is kept at 90% relative humidity. A glass Petri-dish containing tap-water is kept for maintaining humidity. The dry incubator was used for hatchlings.

Characterisation of MNPs in eggs and hatchlings

X-ray micrographs (micro computed tomography, μCT) were obtained on Bruker X-Ray Microtomograph SkyScan 1275 with Source Voltage 40 kV and source Current 220 μA. Scanning electron microscopy-energy dispersive X-ray analysis (SEM-EDX) was performed on Hitachi SU5000 field emission SEM coupled with Oxford Instruments EDX detector in low vacuum mode using back scattered electron detector at 10 kV (similar conditions to that of MNPs characterisation). Raman measurements were performed on Renishaw inVia Qontor® spectrometer using 785 nm laser.

Developmental stages of the egg

For growth study, 2 eggs were kept in each of 21 wells corresponding to a day of the growth (using two 12-well plates). The well-plate was loaded with 300 μL of water, to ensure adequate humidity for growth. Please note that all general glassware (beakers) and plasticware (such as micro well plates, pipette tips) was purchased from Premier Scientific, UK.

MNPs mapping inside locust eggs

Figure S3 shows 1000 $mg.L^{-1}$ MNPs inside the locust eggs. The nanoparticles could not be observed by SEM on the locust surfaces for 10 and 100 $mg.L^{-1}$ MNPs concentration. The main reason why MNPs cannot be seen on the egg surface *via* μCT in the low-loading case is believed to be the very small size of MNPs cluster which may hinder the MNPs appearing in the μCT. μCT resolution depends on the distance

of the object from the X-ray source. For these samples, due to the finite size of eggs and hatchlings, the pixel size (resolution) was around 10 µm. So, any particle smaller than this could not have been seen in the µCT. Regarding SEM analysis of the low MNPs loading, the issue could be the availability of MNPs on the surface and most of them might have been transferred inside the egg.

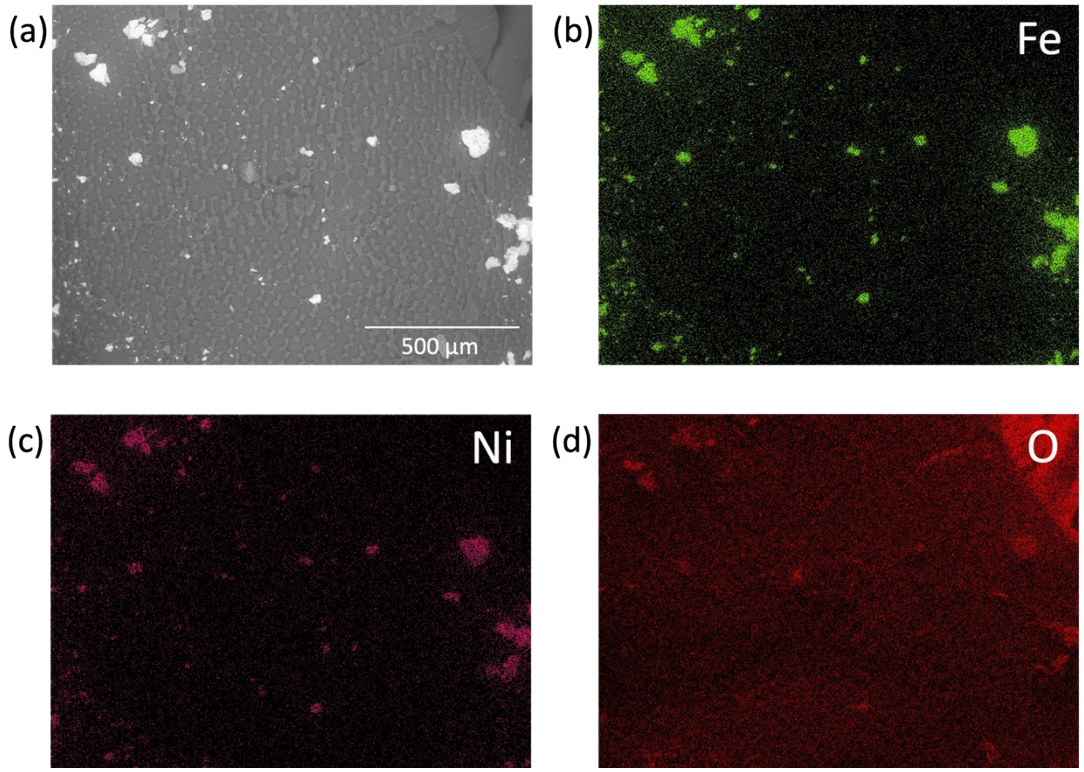

Figure S3. (a) SEM image of skin and corresponding EDX maps for (b) Fe, (c) Ni and (d) O for 1000 mg L^{-1} loading of MNPs on eggs.

Low loading of MNPs allowed the nanoparticles to be transferred to inside egg due to the smaller cluster size. As in case of higher MNPs loading, the cluster size enhanced, resulting in the clusters not being able to pass through the surface pores. This explains why the low loading of MNPs resulted in less hatchlings emerging as compared to higher loading which is further supported by the µCT images.

Locust hatchlings and their consumption behaviour

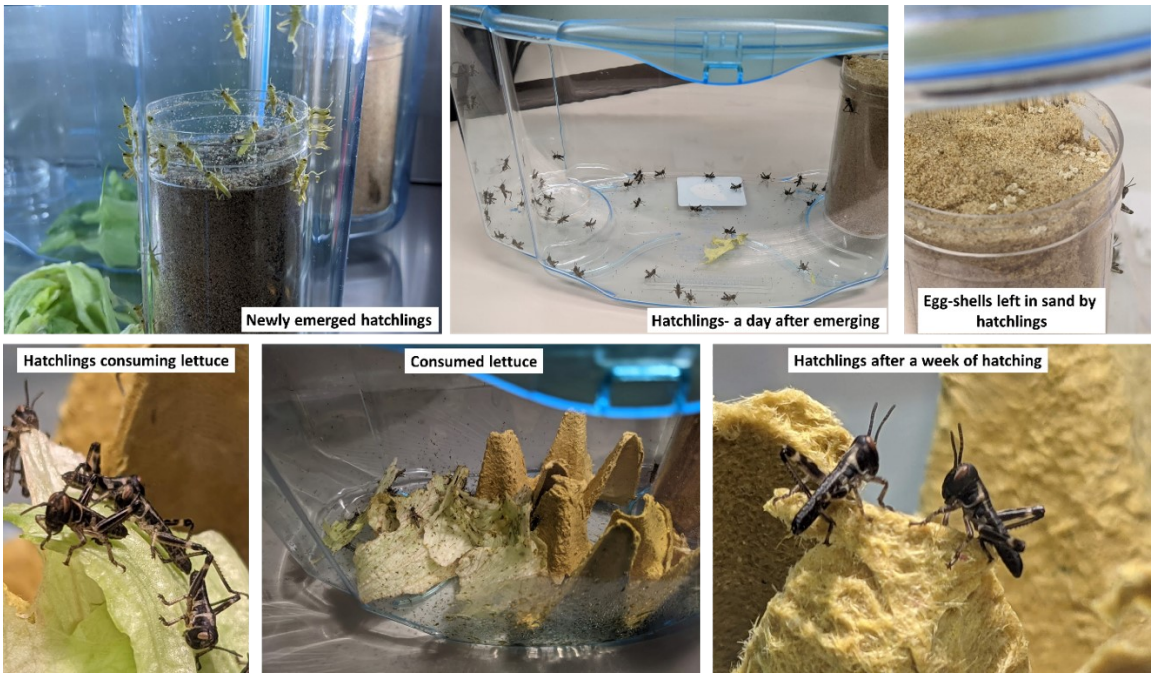

Figure S4. representative images of hatchlings and their feeding in the presence of MNPs. The images are from the batch containing.

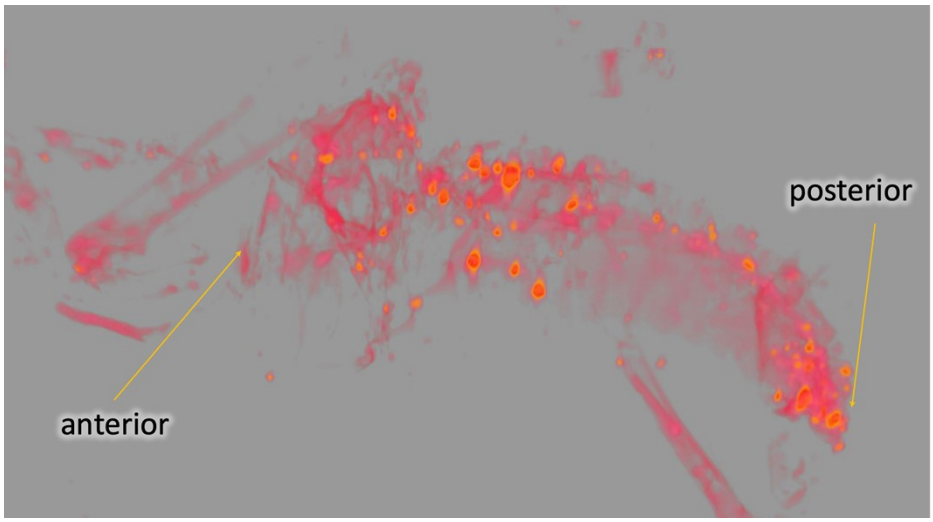

Figure S5. The microCT of a dead nymph after consuming MNPs.

Additional control experiments

Horizontal control

The horizontal controls were performed by keeping the eggs horizontally buried in sand. For this both separated and egg pods were kept in two separate set of experiments. The eggs hatched after 16 days of burying in sand and none of the eggs remained to be hatched. This indicates that the orientation of the eggs does not affect the hatchling.

Egg growth in well plate without sand

The eggs from the jars were taken out in a 12 well plate, 1 to 4 eggs in each well. The eggs did not hatch even after 5 weeks. For some of the eggs, water was added in individual wells (4 wells). None of the eggs hatched. Although, couple of eggs grew slightly which can be seen by the colour transformation (greenish surface) in two of the eggs in the water added wells, however, none of these eggs hatched either.

Recovery of MNPs from sand

Table S1. Recovery of magnetic nanoparticles after multiple cycles

MNPs concentration →	2500 mg/Kg of sand		100 mg/Kg of sand		10 mg/Kg of sand	
	Recovery concentration (average)		Recovery concentration (average)		Recovery concentration (average)	
Cycle ↓	absolute	%	absolute	%	absolute	%
0	2500	100	101	100	11.5	100
1	2465	98.6	100	99.01	10	86.96
2	2442.5	97.7	89.5	88.61	6.2	53.91
3	2358	94.32	83.5	82.67	5.1	44.35
4	2303	92.12	70.3	69.60	4.6	40
5	2274	90.96	71.8	71.09	4.1	35.65

Migration of nanoparticles in sand

The migration of the nanoparticles in the sand was experimentally measured using µCT. The experimentally observed µCT intensities were integrated over till 28 mm depth. It was because after 28 mm, the container had its natural curve and it would have resulted in a false intensity calculations. The µCT concentration of the nanoparticles was normalised with the loaded concentration of the nanoparticles, which is 100 mg L^{-1} in this case.

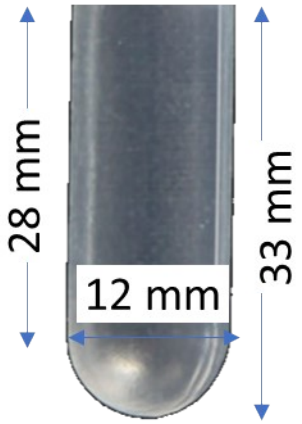

Figure S6. Image and dimensions of the container used for determining NPs concentration in sand.

The intensity data was best fitted using a 2nd order polynomial with the general equation $y = B_2*x^2 + B_1*x + \text{intercept}$. The values of constants were obtained by using the fitting parameters and found that B_2= -6.5 gave the best fit. The physical interpretation of the equation is

$$C_d = - 6.5*d^2 + \text{initial concentration}$$

(equation S1)

Here, C_d is the concentration at depth d.

By inputting different depths and initial concentration, the equation was utilised to give concentration vs depth at various points and is plotted in figure 4h.

Image processing of MNPs in sand

The μCT images at different angles after collection by Bruker mocrotomography instrument, were processed in the Bruker CTVox software. The series of 2D images generate a 3D image in the software. Every point has different intensity in the greyscale point depending on the material and thickness. The software allows selection of grey-scale range and even recolouring. Therefore, depending on the visualisation requirement, either dark or light objects can be removed and recoloured thereafter. In our work. The MNPs appear darker due to the higher atomic weight of the elements of the MNPs compared to sand. Therefore, after the μCT, the lighter greyscale was removed to remove shades corresponding to sand and polystyrene container. This enabled the visualisation of only MNPs.